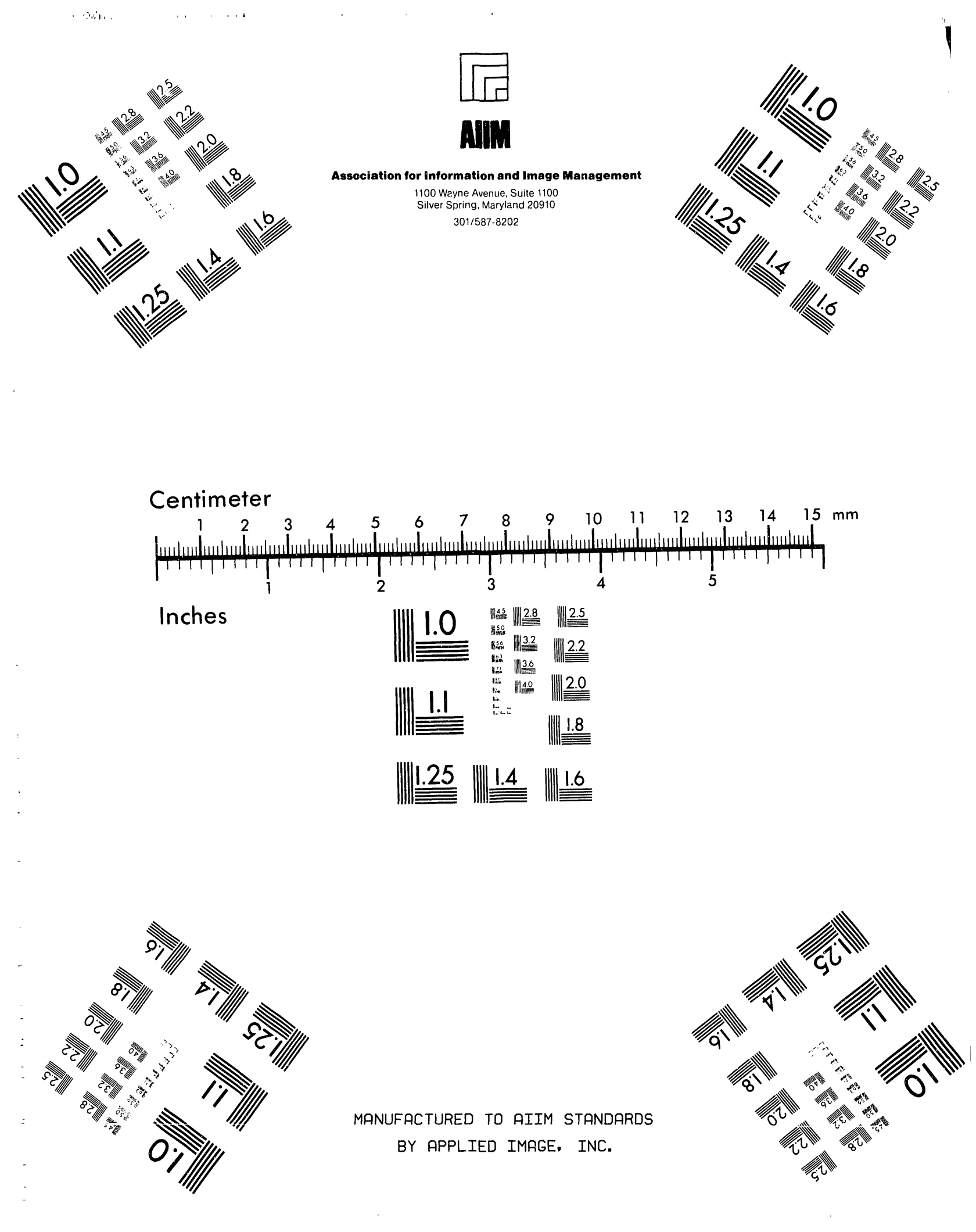
AIIM
Association for information and Image Management
1100 Wayne Avenue, Suite 1100
Silver Spring, Maryland 20910
301/587-8202
Centimeter
Inches
MANUFACTURED TO AIIM STANDARDS
BY APPLIED IMAGE, INC.

1 of 1

INTERPRETATION OF RISK SIGNIFICANCE OF PASSIVE COMPONENT AGING USING PROBABILISTIC STRUCTURAL ANALYSIS[1]

EGG-M-93123

Jerry H. Phillips[2]
Tenera, L.P.
Idaho Falls, Idaho

Corwin L. Atwood
Idaho National Engineering Laboratory
EG&G Idaho, Inc.
Idaho Falls, Idaho

ABSTRACT

The probabilistic risk assessments (PRAs) being developed at most nuclear power plants to calculate the risk of core damage generally focus on the possible failure of active components. Except as initiating events, the possible failure of passive components is given little consideration. The NRC is sponsoring a project at INEL to investigate the risk significance of passive components as they age. For this project, we developed a technique to calculate the failure probability of passive components over time, and demonstrated the technique by applying it to a weld in the auxiliary feedwater (AFW) system. The selection of this component was based on expert judgment of the likelihood of failure and on an estimate of the consequence of component failure to plant safety. We used a modified version of the PRAISE computer code to perform a probabilistic structural analysis to calculate the probability that crack growth due to aging would cause the weld to rupture. We modified an existing PRA (NUREG 1150 plant) to include the possible rupture of the AFW weld, and then we used the weld rupture probability as input to the modified PRA to calculate the change in plant risk with time. The results showed an insignificant effect on plant risk because of the low calculated rupture rate of the weld in this particular calculation over 48 years of service. However, the most interesting observation was the rupture rate trend for this 48 years. A decreasing yearly rupture rate for this weld was calculated instead of the increasing rupture rate trend one might expect. We attribute this result to infant mortality; that is, most of those initial flaws that will eventually lead to rupture will do so early in life. This means that although each weld in a population may be wearing out, the population as a whole can exhibit a decreasing rupture rate. This observation has implications for passive components in commercial nuclear plants and other facilities where aging is a concern. For the population of passive components that exhibit a decreasing failure rate, risk increase is not a concern. The next step of the work is to identify the attributes that contribute to this decreasing rate, and to determine any attributes that would contribute to an increasing failure rate and thus to an increased risk.

I. INTRODUCTION

Probabilistic risk assessments (PRAs) are being developed at most nuclear power plants to determine the risk of core damage. These assessments do not consider aging of the plant's hardware, and give little consideration to the failure of passive plant components; their failure probability is low compared to that of active components, and the large number of these components makes analysis difficult. However, there is some concern that the failure probabilities for these passive components may be increasing as the components age. This concern might be valid. Then, because of the large number of passive components (many feet of pipe, numerous welds, numerous valve bodies, etc.) in a plant, and the potentially large consequences associated with component failure, it is important that aging passive components be considered when an estimate of the risk of core damage is determined for the plant.

The Aging Risk of Passive Components Project being conducted at the Idaho National Engineering Laboratory (INEL) is part of the Nuclear Plant Aging Research Program sponsored by the United States Nuclear Regulatory Commission (USNRC). The objective of the project is to develop ways of determining the effect of the aging of passive components on the risk of core damage in light water reactors.

Our effort included (a) the development of criteria for selecting important passive components for analysis, (b) the adaptation and use of probabilistic structural analysis techniques for calculating the probability of failure of these components with component age, and (c) the inclusion of the results of that analysis in a modified PRA to determine the effects of passive component aging on the risk of core damage. We have demonstrated the techniques by

[1]Work sponsored by the United States Nuclear Regulatory Commission, Office of Nuclear Regulatory Research, under Contract No. DE-AC07-76ID01570. Dr. G. H. Weidenhamer, NRC technical monitor.

[2]Formerly with the Idaho National Engineering Laboratory.

selecting for analysis a weld in the auxiliary feedwater (AFW) system, applying probabilistic structural analysis to the weld, and including the results in the modified PRA.

We believe the insights gained from this project will result in the development of a procedure that can be applied to passive components in nuclear power plants. The procedure should prove useful in selecting components for analysis, evaluating their risk significance, and prioritizing them for the plant in-service inspection program.

This paper focuses on the results of the probabilistic structural analysis of the AFW weld. Section 2 explains the selection of the weld in the AFW system for analysis and discusses our use of probabilistic structural analysis in calculating the failure probability of a passive component, Section 3 discusses the interpretation of these results, and Section 4 presents conclusions and recommendations.

II. SELECTION OF COMPONENT, AND PROBABILISTIC STRUCTURAL ANALYSIS TECHNIQUES USED

This section briefly describes the passive component selected, the risk significance of the component, the transients and stresses affecting the component, and the probabilistic structural analysis code used in this study.

Criteria for Component Selection

The criteria for selecting the passive component for evaluation are based on risk. Specifically, these criteria are as follows: (a) the component must be in a risk-significant system (the component must be a part of a system with large importance), and (b) the component must have an identified or potential aging mechanism that could cause the estimated failure probability to be high or increasing. In addition, for this project, a third criterion was considered: computer programs and calculational techniques must already be available for calculating the probability that the identified aging mechanism will cause failure (resources to develop new tools for probabilistic structural analysis were not available).

Selection of the Component—Auxiliary Feedwater Piping Weld

The component selected for evaluation in this study is an AFW piping weld downstream of the check valve that separates the main feedwater system from the AFW system, and the failure mode is rupture. The rupture of a pipe in the AFW system can lead to loss of portions or all AFW if not recovered by operator action. For this study, rupture of the weld downstream of the check valve is assumed to have the same consequences as rupture of a pipe in the AFW system. Because the AFW system is an important system in the mitigation of most accident scenarios in the PRA (Schmidt et al., 1985), failure of portions or all of this system will have a significant effect on the core damage frequency. Thus, the first selection criterion is satisfied. Rupture is postulated to be caused by fatigue, an aging mechanism observed by Shah and MacDonald (1989); thus, the second criterion for component selection is satisfied. Probabilistic structural analysis computer codes are available to calculate the probability of rupture caused by fatigue; thus, the third criterion is satisfied.

To confirm the importance of the AFW weld to plant safety, we modified a PRA and determined the effect of rupture of the weld on the core damage frequency; see Phillips et al. (1992). Figure 1 is a plot of the unrecovered weld rupture frequency versus the core damage frequency. It can be seen that a weld rupture frequency of greater than about 10^{-5} starts to increase the core damage frequency. The weld therefore satisfies criterion 1 above.

The original design analyses anticipated that the AFW piping would be subject to thermal fatigue caused by transients such as heatup/cooldown cycles and reactor scram; however, cycles of thermal fatigue caused by leaking check valves and stop valves were not anticipated. Postulating such unanticipated thermal cycles due to check valve leakage is reasonable because check valve leakage is well known as a likely occurrence. A recent study by Greenstreet et al. (1985) addressing aging of check valves shows from operating experience records that the dominant failure mode is reverse leakage past the check valve seating surfaces. Fifty-two percent of the failed check valves had reverse leakage. The study reports a search of the NPRDS (Nuclear Plant Reliability Data Systems) database showing that of 382 plant events, 70% involved seat leakage in check valves. Leaking check valves are common events that can cause thermal fatigue. Therefore the weld satisfies criterion 2.

The Transients Causing Component Stress

Figure 2 shows the configuration of the AFW system at an operating commercial power plant. Thermal transients caused by check valve leaks have been observed at operating commercial power plants. If reverse leakage occurs through several check valves in a series all the way to one of the AFW pumps, steam binding can occur in the pump.

If only the first check valve leaks, as was assumed in this study, a circulatory flow between the feedwater lines can occur. The circulatory flow is caused by differences in pressure in the different

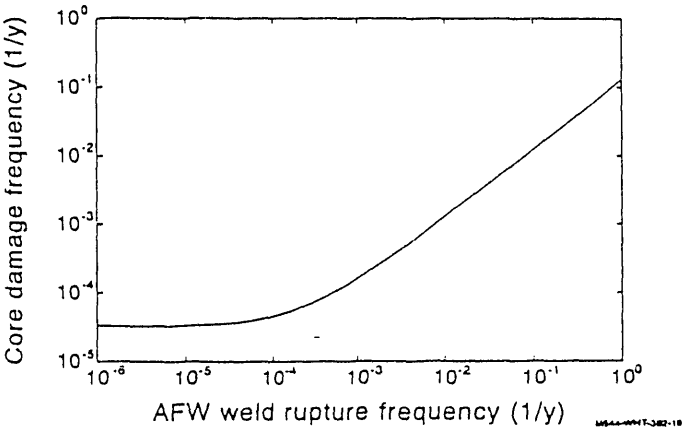

FIGURE 1. UNRECOVERED WELD RUPTURE FREQUENCY VERSUS CORE DAMAGE FREQUENCY.

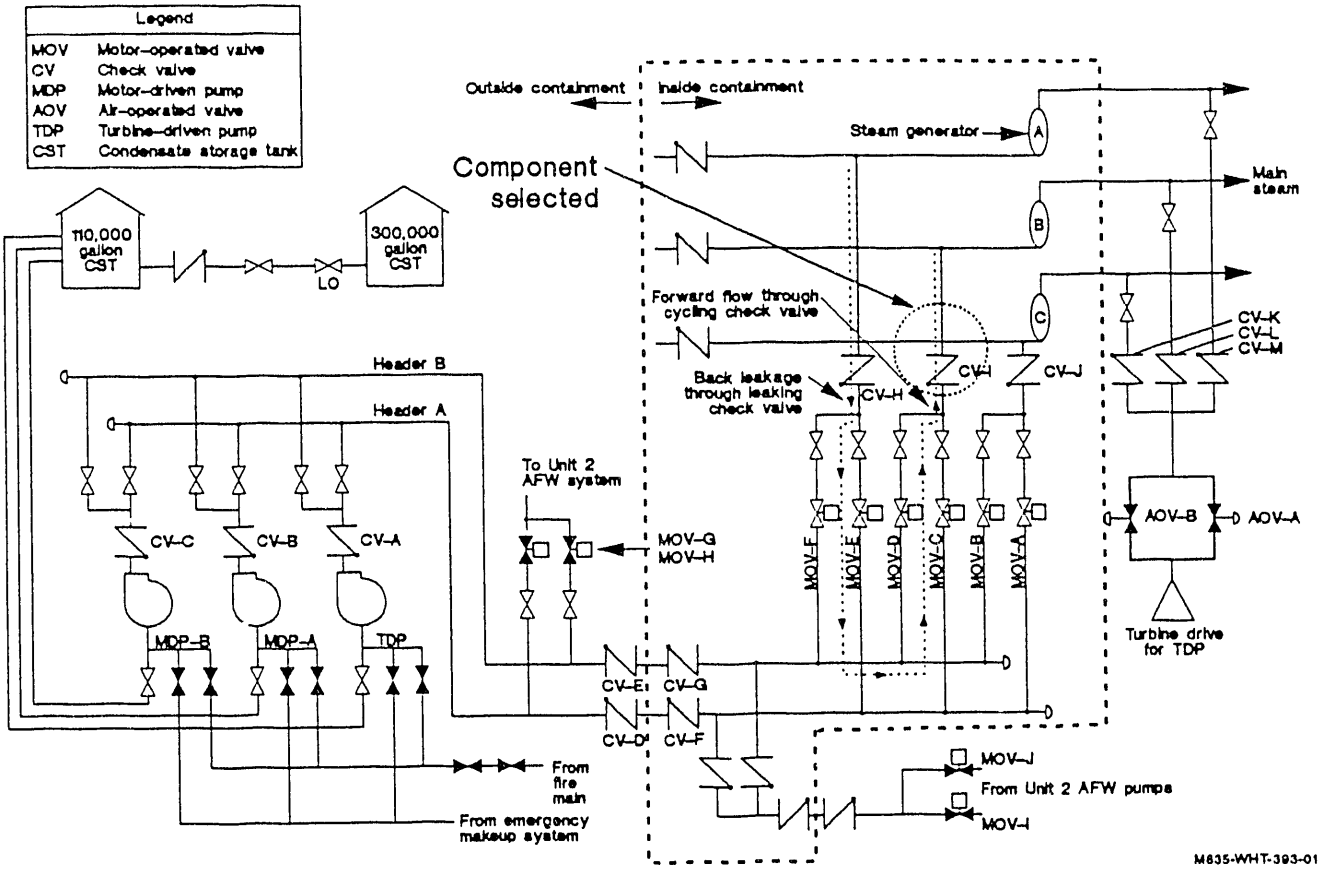

FIGURE 2. SIMPLIFIED DIAGRAM OF AN AFW SYSTEM, SHOWING THE LOCATION OF THE WELD.

feedwater lines. These differences are caused by differences in feedwater piping lengths, differences in steam generators, etc. The pressure difference is thought to be less than or equal to 10 psi (69 kPa). The pressure differences among the feedwater lines causes reverse leakage through one check valve into the AFW system and forward leakage through a second check valve into another feedwater line. The forward leakage causes the second check valve to cycle open and closed; pressure builds up behind the disk until it forces the valve open, then drops until the disk closes again, intermittently exposing the normally hot weld downstream of the check valve to cooler water. Less than 1 psi (6.9 kPa) pressure difference is necessary to open the check valve in the forward direction. As described by Reeves (1988), cyclic flow, similar to the transient just described, caused a safety injection line at the J. Farley Nuclear Plant to crack. In that case, the flow rate through the leaking check valve was estimated at one gallon (3.8 L) per minute.

The specific area of the piping chosen for analysis (circled on Figure 2) is the weld on the downstream side of the cycling check valve. We assumed that this weld is kept relatively hot because of natural circulation of hot water in the feedwater pipe. The weld rapidly cools as cooler water from the AFW system sweeps by the weld when the check valve cycles open. When the check valve closes, the weld slowly heats as natural circulation resumes. The water in the AFW system is cooler because the hot water that enters the AFW system through the leaking check valve has time to cool before it exits through the cycling check valve, assuming slow leakage into the AFW system and heat loss to ambient. The cooler water produces thermal cyclic stresses as it sweeps past the hotter weld.

Stress Caused by the Transient

Stresses on the AFW pipe are caused by the cyclic mechanism described above, as well as by piping design loads, heatup and cooldown of the reactor coolant system, and rapid cooling of the pipe during AFW initiation following a scram. The magnitude and rate of the cyclic stress in the weld are very complicated, depending on many parameters, such as rate of back leakage through the check valve, pressure difference in the feedwater lines, length of piping, amount of insulation on the piping, and orientation of the piping.

Using our best estimate of these parameters, and using as guidance the published evaluation of similar transients in other nuclear piping systems (USNRC, 1988), we calculated the stresses from the cyclic transient using the Tiffany code (Dedhia et al., 1982). The Tiffany code calculates the fracture-mechanics parameters for input into the probabilistic structural analysis. We assumed the frequency of check valve cycling to increase as leakage into the AFW system increases. The rate was obtained from the Reeves report

(1988) on the Farley incident, and the period of the cycles was assumed to be 20 minutes initially, decreasing gradually to 2 minutes over 20 years, and then remaining constant at 2 minutes. We also used the Tiffany computer code to calculate the through-wall stresses from the initiation of the AFW system during a reactor scram.

We used the ASME code-allowable stresses for the conditions of dead weight, pressure, and thermal expansion (heatup and cooldown). These stress values are as follows:

Dead weight stress—1.2 ksi (8.3 MPa)

Pressure stress—3.42 ksi (23.6 MPa)

Thermal expansion stress—22.5 ksi (155.1 MPa).

Selection and Adaptation of Probabilistic Structural Analysis Computer Code

Probabilistic structural analysis techniques calculate the failure probability from stress and strength distributions. Figure 3 shows these distributions; the overlap area, shaded, is an indication of the failure probability of a passive component. As the stress and strength distributions spread and shift with time, the overlap area can get larger. An increase in the overlap area would be an indication of increased failure probability caused by aging.

We searched for a probabilistic structural analysis code to perform the failure analysis. Several commercial codes were reviewed, along with some codes developed by national laboratories. The advantage of a code developed by a national laboratory is that the source code is generally available. We needed the source code so we could make changes in the code to account for aging. We selected the Piping Reliability Analysis Including Seismic Events (PRAISE) code to perform the calculations on the AFW piping weld because the source code was available, the code is widely used, and the code is applicable to the component selected.

Developed at Lawrence Livermore National Laboratories (LLNL), PC-PRAISE is the PC version of PRAISE-C, which is a mainframe version of PRAISE. As described in Harris et al. (1992), PRAISE is a probabilistic fracture mechanics code that models the growth of piping flaws by anticipated or accidental stresses during the operation of a nuclear power plant. When these flaws grow (in the model) to certain critical levels, they cause the pipe to leak or catastrophically break. PC-PRAISE retains all the features of the original PRAISE and has the capability to model stresses and failure mechanisms other than cyclic fatigue, such as stress corrosion cracking, residual stresses, and vibration stresses.

Figure 4, duplicated from Harris et al. (1981), shows the different modules in PRAISE. The starting point (module A) is the initial crack depth and crack aspect ratio (which are input by the user). The crack is assumed to have two-dimensional, semielliptical geometry; the length of the crack is $2b$, the depth is a. The pipe wall thickness is h. The cracks can grow in both length and depth. As they grow, there is a possibility that they will be detected and corrected. The crack nondetection probability distribution is represented by Module B in Figure 4. This nondetection distribution combines with the initial crack size distributions to give the post

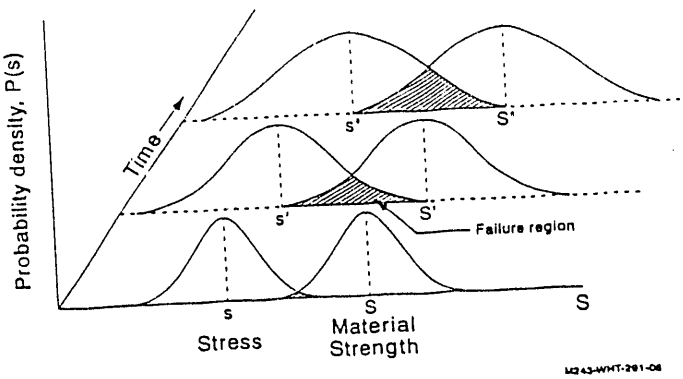

FIGURE 3. STRESS AND STRENGTH DISTRIBUTIONS; THE OVERLAP AREA (STRESS STRENGTH INTERFERENCE) CAN CHANGE WITH PLANT AGE.

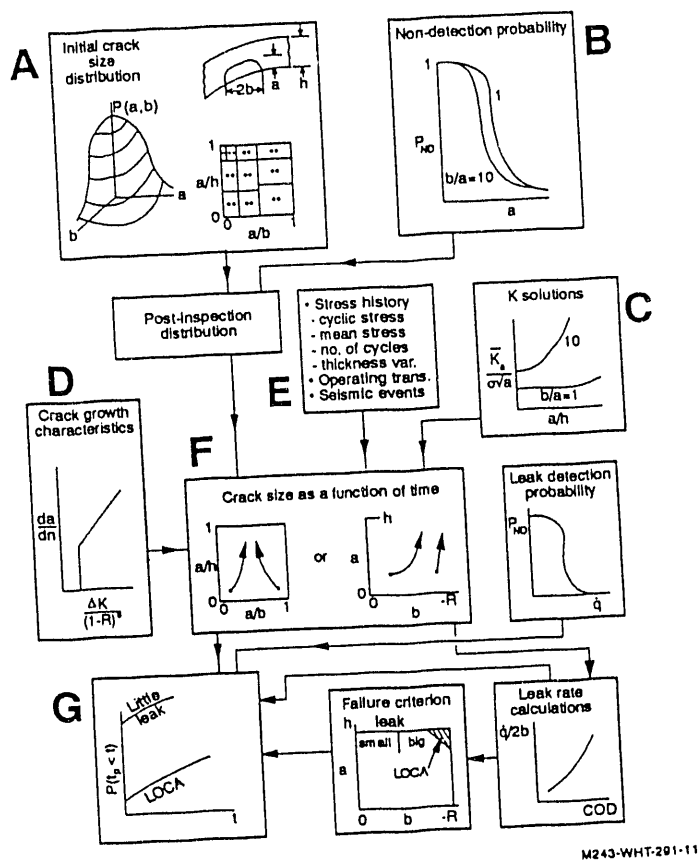

FIGURE 4. STEPS TAKEN USING PRAISE IN THE PROBABILISTIC STRUCTURAL ANALYSIS OF THE AFW WELD (HARRIS ET AL., 1981).

inspection distributions. For this study, we assumed that a crack would be detected if and only if the leak rate was as large as 5 gallons (19 L) per minute. The postinspection distributions, in turn,

... Module F, which calculates crack size as a function of ... information needed for the crack growth calculation, ... the crack growth curve (Module D), K-solution (Module ... the stress history (Module E), are also input into Module F. ... output from Module F is the new crack size. Module G com- ... the conditional cumulative failure probability by modifying the new crack size distribution to account for leakage detection and then "overlapping" this filtered distribution with the failure crite- ... distribution. This last step resembles an application of stress- ... gth interaction (see Figure 3). Thus, PRAISE can be called ... a stress strength interaction code or a probabilistic structural ... lysis code.

... huge and complex computer code such as PRAISE can be ... cult to use. We relied on Lawrence Livermore National Labo- ... ates Failure Analysis Associates (consultant to LLNL), and others for assistance in the task of modifying the code and develop- ing input for the analysis.

Ellyin (1985) has addressed fatigue as an aging mechanism in probabilistic studies. However, few of the associated studies addr... the increasing fatigue rate or the changes that occur in the stress and strength distributions over time, which result from changes in the thermal cycle rate and from changes in the material properties caused by aging.

We modified the PRAISE source code to account for the aging-induced changes in material properties and for a varying transient cycle rate over the life of the component. Modifications were also made to provide intermediate output, so that changes in failure probability could be measured at selected times during the life of the plant.

We searched the literature for material-properties changes to determine how material parameters such as yield strength, ultimate tensile strength, dJ/da (unstable crack growth parameter), and da/dn (fatigue crack growth), would change as plant components age. Because changes in material properties of interest occur over long periods (40 years and greater), limited material property data could be found. We attempted to estimate, based on expert judgment, many of these changes with age.

III. INTERPRETATION OF RESULTS OF THE PRAISE CALCULATIONS

Effect of Any One Initial Flaw Size

Several possible events can terminate the life of the weld. PRAISE considers that the weld will be taken out of the pipe if the weld fails the preservice hydrostatic proof test, if a leak occurs that is large enough to be detected, or if a rupture occurs; "termination" is used here to include these three kinds of events. For this study, a nonrupture leak was considered detectable if the leak rate was as large as 5 gallons (19 L) per minute.

Figure 5 shows the region of initial flaws considered in this study, with a, b, and h as defined in Figure 4. Aspect ratios a/b greater than 1.0 were not considered; this is conservative, because such large aspect ratios would not lead to rupture. The left side of Figure 5 is not quite rectangular; this is caused by the geometrical constraint that $2b$ cannot be larger than the inner circumference of

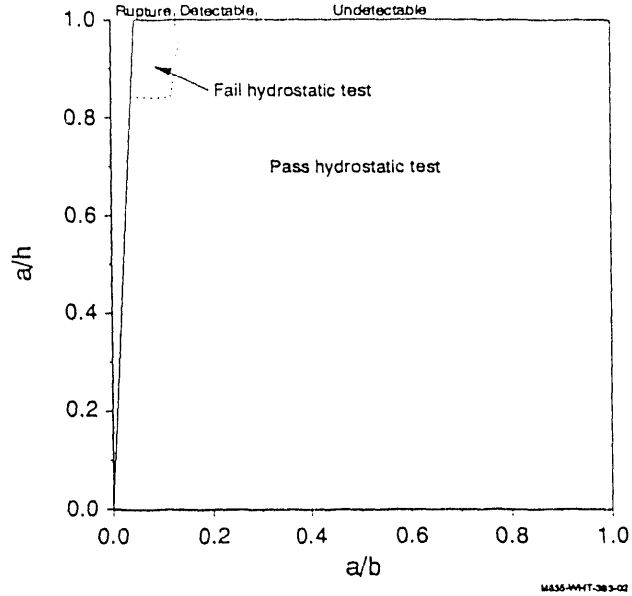

FIGURE 5. DIMENSIONS OF INITIAL FLAWS THAT EITHER PASS OR FAIL THE PRESERVICE HYDROSTATIC TEST.

the pipe. When $a/h = 1.0$ in Figure 5, the flaw has penetrated the weld thickness. The portions of the line $a/h = 1.0$ that correspond to an undetectable leak (<5 gpm), a detectable leak (≥ 5 gpm), and a rupture are marked. The boundaries between these three line segments were determined from simulations, by running PRAISE with flaws having $a/h \doteq 1.0$ and having various values of a/b. (Because of randomness in the material properties, the boundaries have a slightly random component to them, but this is too minor to be visible in the figure.) These boundaries do not change as the weld ages, because the assumed aging material properties vary only slightly with time. Also shown in the figure is the region where the weld would fail the preservice hydrostatic proof test. This region was also determined from simulations, by running PRAISE with various welds with flaw dimensions in the upper left corner of the figure. It can be seen that PRAISE's simulation of the hydrostatic proof test successfully detects flaws that would have caused immediate rupture.

Now consider how a flaw grows over time. Figure 6 shows the paths of selected flaws as they grew for 48 years. The initial values of a/h and a/b were regularly spaced on a 10×10 grid. On any one path, the open square marks the point (a/b, a/h) before the hydrostatic proof test. The solid circles mark the points at time 0 (i.e., immediately after the hydrostatic proof test), and at 8, 16, 24, 32, 40, and 48 years. If the weld is terminated before 48 years, either by a detectable leak or a rupture, the point (a/b, a/h) is marked by an X and further development of the flaw is not shown.

The speed of growth was not the same for all the flaws, even for flaws with similar initial dimensions, because the rate of fatigue crack growth was chosen randomly for each flaw. This is why some of the tracks have their dots close together (slowly growing flaws) while some nearby tracks have their dots farther apart (faster growing flaws.) The direction of the track is also random to some extent.

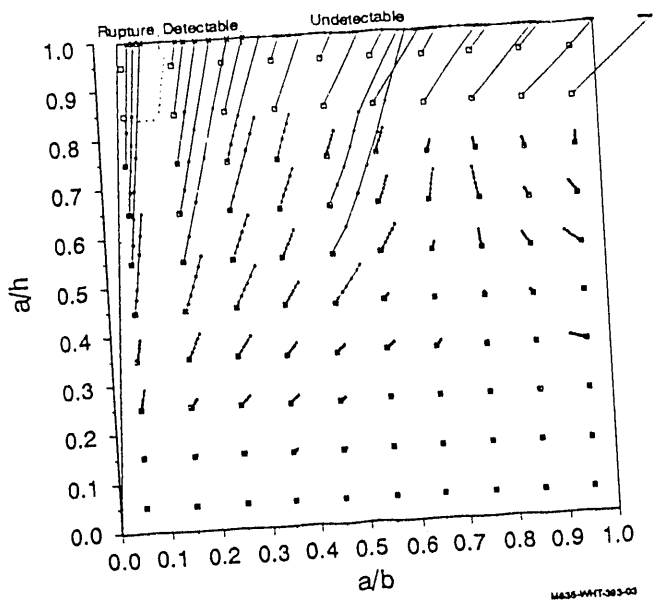

FIGURE 6. FLAW GROWTH TRAJECTORIES DURING THE 48-YEAR LIFETIME OF THE COMPONENT.

In spite of these differences, note several general features of the plot:

- In all but the uppermost portion of the plot, the aspect ratio a/b tends to move towards $a/b = 0.7$. Smaller aspect ratios get larger and larger ones get smaller. Thus, an aspect ratio of 0.7 appears to be the equilibrium flaw size where k (the stress intensity factor) is approximately constant along the crack front.

- Many of the paths seem to radiate directly away from the origin, i.e., the point (0, 0). This is especially the case on the left side of the graph. Such a path satisfies (a/h) = constant $\times (a/b)$, that is, b remains constant while a increases.

- If a flaw ever penetrates the weld as an undetectable leak, it will never cause a rupture. Instead, it will grow until it becomes detectable, at which time the weld will be removed. This progression is called "leak before break."

Consider the second observation in more detail. If a increases but b remains fixed, the track in Figure 6 moves along a vector directly away from the origin. If instead b also increases, the direction vector of the track is rotated somewhat in the counterclockwise direction.

Therefore draw straight lines from the origin to the points at the top of the plot where ruptures, detectable leaks, and undetectable leaks are divided, as shown in Figure 7. Because most paths on the left of Figure 6 move directly away from the origin (i.e., a increases but b hardly changes), the lines in Figure 7 determine the likely destinies of the flaws. Flaws in the region marked "rupture" are initially very long compared to their depth. All flaws starting in

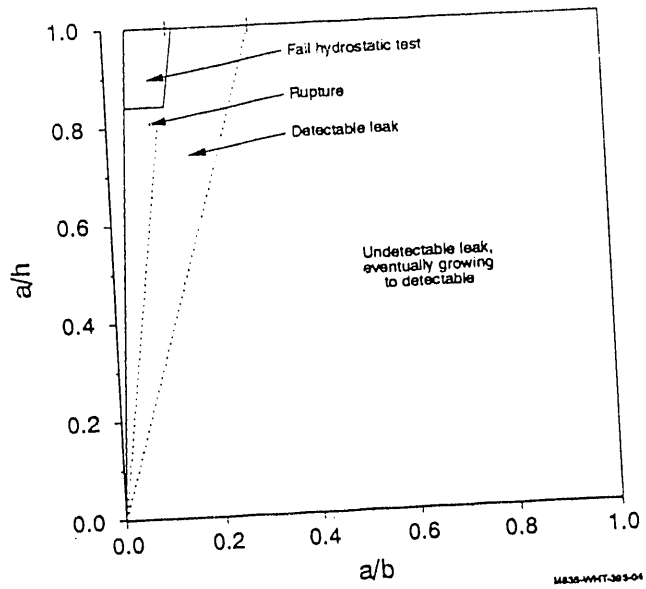

FIGURE 7. LIKELY DESTINIES OF INITIAL FLAWS.

this region must eventually lead to rupture, given enough time to grow. Most flaws in the region marked "detectable leak" will result in detectable leaks, although a few will cross the line into the rupture region. Most of the other flaws will grow to undetectable leaks and then to detectable leaks, although a few will cross the line and be detectable when they first penetrate the wall thickness.

The initial flaws near the top of Figure 7 have initial depth going most of the way through the pipe wall thickness. They result in early penetrations of the weld, either as ruptures, detectable leaks, or undetectable leaks. The initial flaws lower in the figure tend to result in later penetrations of the weld. Consider the wedge-shaped region that leads to ruptures. If a flaw is more likely to be in the broad top part of the wedge than in the narrow bottom part, then early ruptures are more likely than late ruptures. Thus the form of the hazard rate curve, introduced below, depends both on the geometry in Figure 7 and on the probability distribution of initial flaw dimensions, defined next.

Effect of Random Population of Flaw Sizes

The initial flaw dimensions in the weld are unknown, but they follow some probability distribution. A time-dependent probabilistic risk assessment must therefore calculate the probability of rupture in a time period of interest, assuming that the initial flaw was drawn randomly from its distribution. It is assumed that each weld has one flaw; this is probably a conservative assumption.

The probability distributions for initial flaw depth and aspect ratio were those suggested by Schomburg and Schmidt (1984). The flaw depth was assumed to be exponentially distributed with parameter 16.67 in.$^{-1}$, corresponding to a mean of about 0.06 in. (1.5 mm), truncated at the wall thickness of 0.216 in. (5.5 mm). That is, the density of flaw depth a is

$$\theta e^{-\theta a}/(1-e^{-\theta h}),\ \theta = 16.67,\ h = 0.216,\ 0 \le a \le h \quad . \tag{1}$$

Therefore a/h also has a truncated exponential distribution, shown in Figure 8. Note that this assumed density decreases monotonically in a, so that shallow initial flaws are more likely than deep initial flaws.

The inverse aspect ratio of the initial flaw, b/a, was assumed to have a shifted exponential distribution: $(b/a - 1)$ has an exponential distribution with parameter of 0.689. This is one of two distributional forms suggested by Schomburg and Schmidt (1984) and allowed by PRAISE, the other being lognormal. An exponential density $\theta e^{-\theta y}$ for $y = b/a - 1$ can be shown to correspond to the density $\theta x^{-2} e^{-\theta(1/x-1)}$ for $x = a/b$, $0 < x < 1$. (See Mood et al., 1974.) This density of a/b is also shown in Figure 8. It is very small near 0, and has a single mode at $\theta/2$, which equals 0.3445 for the assumed θ. Smaller aspect ratios and larger aspect ratios are less likely than aspect ratios near 0.3445.

The distributions of a and b/a were assumed to be statistically independent, as suggested by Harris et al. (1992); therefore, the distributions of a/h and a/b were statistically independent.

To increase the efficiency of the simulations, the upper left portion of Figure 7 was divided into 88 square cells, covering about half of the figure, and within each cell 500 or 1000 initial flaws were generated, according to the conditional probability distribution of flaws within the cell. Cells more likely to produce rupture had 1000 simulations each, while those that would produce only detectable leaks had 500 simulations each, for a total of 76,000 simulated initial flaws. Each resulting weld was then simulated until it terminated or for 48 years, whichever came first. This sampling by cell is called stratified sampling, and it is much more efficient than simple random sampling for studying events such as ruptures that occur only in a region of low probability.

Probability of Rupture

A very relevant quantity for a PRA is

Prob[rupture this year, at a weld that is in its nth year]

= Prob[rupture in year n | no termination before year n]

= Prob[rupture in year n] / Prob[no termination before year n] . (2)

Here, the vertical line denotes conditional probability: Prob [A | B] is the probability of A given B. Recall that the weld is terminated if it fails the preservice hydrostatic test, if a leak occurs that is large enough to be detected, or if a rupture occurs.

The probability of a rupture during any t hours in year n can be found by multiplying Expression (2) by $t/8760$. Expression (2) is now estimated using the quantities defined next. We could begin with the annual probabilities or the cumulative probabilities, but PRAISE prints the cumulative probabilities, so we begin there. Define the *cumulative distribution function* for termination (end of weld life) as

$F_{term}(t)$ = Prob(termination at or before time t)

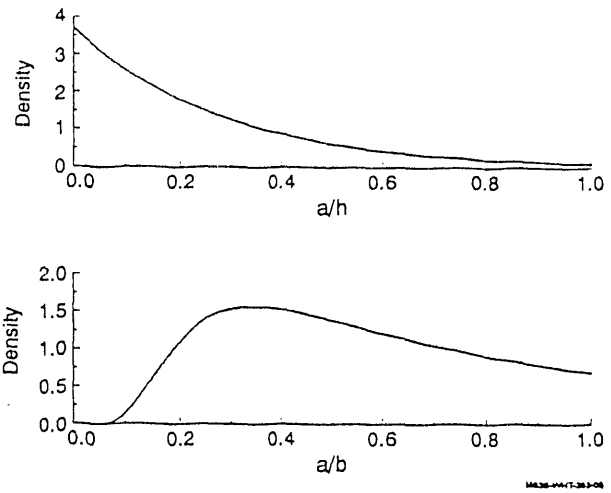

FIGURE 8. DENSITIES OF a/h (FLAW DEPTHS) AND a/b (FLAW ASPECT RATIOS) USED IN THIS STUDY.

and define $F_{rupture}(t)$ similarly. These cumulative distribution functions are estimated at the end of each year, based on the number of simulated terminations or ruptures in each of the cells. The formulas are standard; see Section 7.3 of Harris et al. (1992).

Figure 9 shows the estimated cumulative probability of rupture, as calculated by PRAISE. These calculations included inputs for material properties that changed over time. Including these changes in the material properties made a negligible change in the results, but it did lengthen the computation time by more than an order of magnitude.

The heavy line in Figure 9 is the estimate of $F_{rupture}(t)$, and the two thinner lines show the estimate $\pm 2\,\sigma$. Here σ is the standard deviation of the estimate of $F_{rupture}(t)$, resulting from the Monte Carlo sampling of the initial flaw sizes, the material properties of the welds, and the stresses over time. The formulas for calculating σ are given in Section 7.3 of Harris et al. (1992).

Similarly, Figure 10 shows the estimated $F_{term}(t) \pm 2\,\sigma$. Note that $F_{term}(0)$ is greater than zero, reflecting the fact that 0.34% of the simulated welds failed the preservice hydrostatic test or developed detectable leaks during the initial transient.

Now define the *density* $f_{rupture}(t)$ by

$$f_{rupture}(t) = (d/dt)F_{rupture}(t) \quad .$$

For a time t in year n, we have $n-1 \le t \le n$, and $f_{rupture}(t)$ is estimated by

$$\Delta F_{rupture}(t) \equiv F(n) - F(n-1) \quad .$$

Therefore, $f_{rupture}$ is estimated as a constant within any one year, the slope of the piecewise linear function in Figure 9. Finally, define the *generalized hazard* rate as

$$\lambda_{rupture}(t) = f_{rupture}(t) / [\,1 - F_{term}(t)\,] \quad .$$

This definition generalizes the ordinary hazard rate, for which the numerator and denominator refer to the same kind of event. The

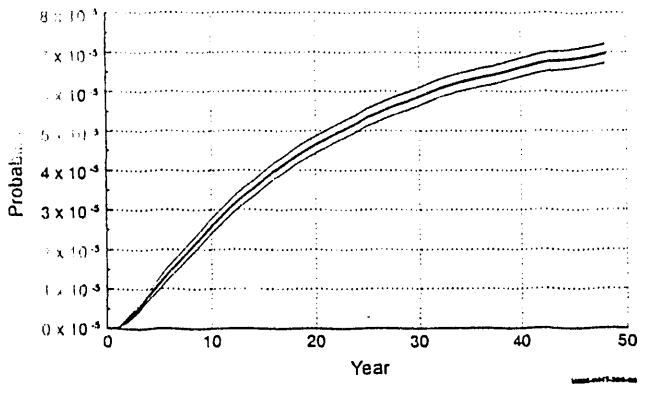

FIGURE 9. CUMULATIVE RUPTURE PROBABILITY FOR THE WELD, WITH A SLOPE THAT INDICATES A DECREASING HAZARD RATE LATER IN COMPONENT LIFE.

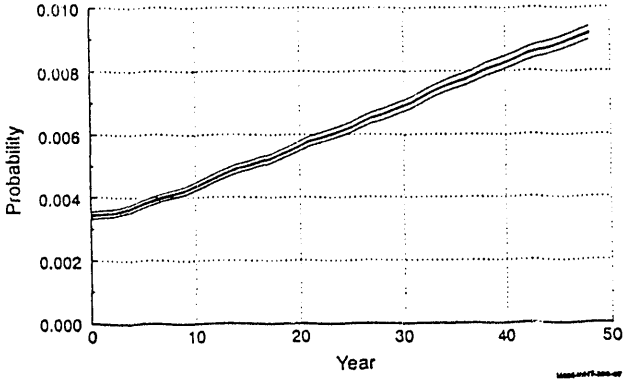

FIGURE 10. CUMULATIVE PROBABILITY OF TERMINATION OF THE WELD, WITH THE SLOPE INDICATING A CONSTANT RATE.

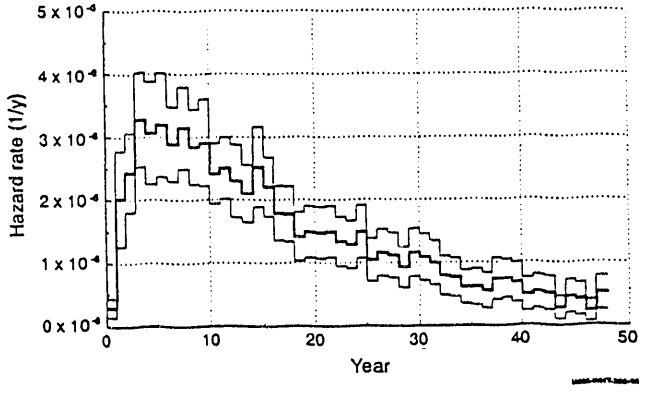

FIGURE 11. GENERALIZED HAZARD RATE FOR RUPTURE BY YEAR, INDICATING A DECREASE WITH AGE.

desired quantity given by Expression (2) is $\lambda_{rupture}(t)\Delta t$ with Δt equal to one year. This is estimated by

$$\Delta F_{rupture}(t) / [\, 1 - F_{term}(n-1) \,] \quad . \tag{3}$$

Note from Figure 10 that $1 - F_{term}(t)$, which is the denominator in $\lambda_{rupture}$, is always greater than 0.99. Therefore, $\lambda_{rupture}(t)$ is virtually equal to $f_{rupture}(t)$, for $t \leq 48$ y. The inaccuracy is at most about 1%, which will be seen to be negligible compared to the Monte Carlo error bounds on $\lambda_{rupture}$. Figure 11 shows a plot of the estimated generalized hazard rate $\lambda_{rupture}$. This figure plots Expression (3), and is the estimator of Expression (2).

The error bounds reflect the fact that the inputs to PRAISE were chosen by Monte Carlo sampling. The heavy line is the average of the PRAISE outputs, and at any time t the upper and lower limits form an approximate 95% confidence interval for the estimated quantity. If many more Monte Carlo runs had been made, the heavy line would stabilize to a nonrandom line, and the width of the error band would shrink to zero. The error bounds reflect only Monte Carlo variation, not any of the existing uncertainty about the correct inputs to PRAISE. If a variety of plausible distributions had been used for initial flaw size, material properties, cycle rate, etc., wider bounds could be constructed that include uncertainty about the true distributions.

Interpretation and Explanation of the Hazard Rate

The generalized hazard rate in Figure 11 shows a sharp increase, followed by a prolonged decrease. Although there is some roughness in the plot, resulting from the random Monte Carlo simulations, the general shape of the curve is clear. It cannot be attributed to random error in the Monte Carlo sampling, but would be seen even if many more runs of PRAISE had been made. Reasons for this behavior are given in the following discussion.

First consider the increase in the early years. As discussed in connection with Figure 5, the hydrostatic proof test successfully detects flaws that would have caused immediate rupture, and largely eliminates ruptures in the first year. This is the apparent cause of the initial small hazard rate.

Flaws not found during the hydrostatic test but whose dimensions predispose them to early rupture account for the sharp increase in the hazard rate during the first few years.

Now consider the decrease after the early years. The decrease may seem paradoxical, because one would think that each weld has an increasing hazard function, because flaws can grow but they cannot shrink. The explanation lies in the way simulated flaws grow under the assumed conditions, and the fact that Figure 11 shows the rupture rate not for a single flaw but for a flaw drawn randomly from a population. Figure 7 showed that most initial flaws do not result in ruptures at all, but in detectable leaks instead. The initial flaws that lead to ruptures are all in or very near the wedge-shaped region labeled "rupture" in Figure 7. If the top part of that region has higher probability than the middle or bottom part, then early ruptures are more likely than late ruptures. This is what happens in our case.

It seems possible to change the assumptions about the stress gradient so that the hazard rate for ruptures would increase: (a) change the assumptions about the stresses, so that the tracks in Figure 6 move toward the left instead of toward the right; or (b) change the probability assumptions so that the region of Figure 7 yielding late ruptures has higher probability than the region

yielding early ruptures; or (c) change the material properties radically over time, so that the rupture portion of the top line becomes noticeably larger as time passes. Further investigations should consider which changes of these types can be considered realistic. Dedhia et al. (1983) have investigated the effect of combinations of thermal and bending stresses, and reached conclusions similar to those of this paper.

It is fairly common in reliability settings to find that a population of components has a decreasing hazard rate even if none of the individual components has a decreasing hazard rate. See, for example, Proschan (1963) and Evans (1992). Thus, it should not be surprising to find the phenomenon in the present context. The high early hazard comes from items with large initial defects. If a component survives past infancy without failing, it is probably a well-made component, with every hope of a long life.

This simulation considered only one degradation mechanism (fatigue). In an examination of passive component data bases that document failures from many degradation mechanisms, Thomas (1981) likewise observed a decreasing hazard rate. Thomas's finding indicates that some populations of passive components show trends similar to the trend observed in this study.

IV. CONCLUSIONS

The results indicate the value of using a probabilistic structural analysis tool such as PRAISE. The hazard rate trends can be determined as a function of time. We were most interested in rupture, which would result in the pipe failing to perform its mission—the mitigation of core damage. [Leakage does not affect core damage frequency as long as a sufficient quantity of water can be piped to the steam generators—generally on the order of 600 gallons per minute (38 L/s) from the AFW system.] But hazard rate trends could be determined for leak as well as rupture. One can determine how the detectable leak versus rupture probabilities will change with time. For example, the weld we studied was more likely to leak than to break. Early in life the weld was about 35 times more likely to have a detectable leak than to break; late in the design life it was about 300 times more likely to have a detectable leak than to break.

The hazard rate as a function of time can be applied to the study of aging and its mitigation. Using tools of probabilistic structural analysis, one can investigate and identify the attributes (pipe size, material, transients, stress state, etc.) that would lead to an increasing hazard rate (wear-out). Separate populations can then be identified, one with an increasing hazard rate (which is an aging concern) and the other with a decreasing hazard rate (which is not an aging concern). The hazard rate trends for the population types can be combined with the results of the PRA to create a prioritization scheme based on risk.

The specific findings of these analyses of PRAISE simulations, based on the assumed inputs to the code, are as follows:

1. The cumulative probability of a rupture at the simulated weld in the AFW system is less than 1.0×10^{-4} over a 48-year life.

2. For a flaw with small initial aspect ratio a/b, the value of a tends to grow over time while b remains essentially constant. This pattern is a result of the calculated stresses and flaw growth characteristics.

3. The above pattern of flaw growth, combined with the assumed probability distribution of the initial flaw dimensions, produces a hazard rate $\lambda_{rupture}$ that decreases after the first few years. This is the hazard rate for the population of welds, not for an individual weld, and is the appropriate hazard rate when the true initial flaw dimensions are unknown. The hazard rate per year toward the end of the design life is in the range of 10^{-6}, so the core damage frequency is not changed over time.

4. No calculations have yet been made to study how the above results would change if different credible inputs had been used for PRAISE. Investigation of this issue is necessary if one is to construct a confidence band around the hazard or the cumulative distribution function, with the band reflecting uncertainty about the correct code inputs.

In conclusion, this work has produced some very interesting results using the probabilistic structural analysis tool PRAISE. Logically, the next step in this work is to use this tool and other probabilistic structural analysis tools to identify those attributes that would lead to an increasing hazard rate during the design life of plants.

V. REFERENCES

Dedhia, D. D., Harris, D. O., and Lim, E. Y., 1983, "Influence of Nonuniform Thermal Stresses on Fatigue Crack Growth of Part-Through Cracks in Reactor Piping," in *Fracture Mechanics: Fourteenth Symposium—Volume I: Theory and Analysis*, ASTM STP 791, J. C. Lewis and G. Sines (eds.), American Society for Testing and Materials, pp. I-308 to I-326.

Dedhia, D. D., Harris, D. O., and Denny, V. E., 1982, *Tiffany: A Computer Code for Thermal Stress Intensity Factors for Surface Cracks in Clad Piping.*

Ellyn, F., 1985, *A Strategy for Periodic Inspection Based on Defect Growth, Theoretical and Applied Mechanics*, Vol. 4, pp. 83–96.

Evans, R. A., 1992, "Knowledge *vs.* Understanding," *IEEE Transactions on Reliability*, Vol. *41*, p. 325.

Greenstreet, W. L., Murphy, G. A., Gallaher, R. B., and Eissenberg, D. M., 1985, *Aging and Service Wear of Check Valves Used in Engineered Safety-Features Systems of Nuclear Power Plants, Volume 1: Operating Experience and Failure Identification*, NUREG/CR-4302, p. 51.

Harris, D. O., Dedhia, D. D., and Lu, S. C., 1992, *Theoretical and User's Manual for pc-PRAISE, A Probabilistic Fracture Mechanics Computer Code for Piping Reliability Analysis*, NUREG/CR-5864, UCRL-ID-109798.

Harris, D. O., Lim, E. Y., Dedhia, D. D., Woo, H. H., and Chou, C. K., 1981, *Fracture Mechanics Models Developed for Piping Reliability Assessment in Light Water Reactors*, NUREG/CR-2301, UCRL-15490.

Mood, A. M., Graybill, F. A., and Boes, D. C., 1974, *Introduction to the Theory of Statistics, Third Edition*, New York: McGraw Hill, 1974, Section V.5.1.

Phillips, J. H., Bolander, T. W., Magleby, M. L., and Geidl, V. A., 1992, "Investigation of the Risk Significance of Passive Components Using PRA Techniques," *Fatigue, Fracture and Risk—1992*, ASME PVP-Vol. 241, pp. 91–100.

Proschan, F., 1963, "Theoretical Explanation of Observed Decreasing Failure Rate," *Technometrics, Vol. 5*, pp. 375–384.

Reeves, E., 1988, *Summary of Meeting Held on January 15, 1988, between NRC and APCo Representatives to Discuss Generic Implications of a Cracked Six-Inch Safety Injection Pipe at Farley Unit 2.*

Schmidt, E. R., Jamali, K. M., Parry, G. W., and Gibbon, S. H., 1985, "Importance Measures for use in PRAs and Risk Management," *International Topical Meeting on Probabilistic Safety Methods and Applications*, EPRI NP-3912-SR, Vol. 2, pp. 83-1 to 83-11.

Schomburg, U., and Schmidt, T., 1984, "Probability of Fracture in the Main Coolant Pipe of a Pressurized Water Reactor," *International Union of Theoretical Applied Mechanics Symposium: Probabilistic Methods in the Mechanics of Solids and Structures, Stockholm, Sweden*, New York: Springer-Verlag.

Shah, V. N., and MacDonald, P. E. (eds.), 1989, *Residual Life Assessment of Major Light Water Reactor Components—Overview*, NUREG/CR-4731.

Thomas, H. M., 1981, "Pipe and Vessel Failure Probability," *Third National Reliability Conference—Reliability 1981*, pp. 3C/4/1 to 3C/4/14.

U.S. Nuclear Regulatory Commission, *1988, Thermal Stresses in Piping Connected to Reactor Coolant Systems*, NRC Bulletin 88-08.

DATE
FILMED
8/4/93

END